Complex Planetary Systems II: Latest Methods for an Interdisciplinary Approach
Proceedings IAU Symposium No. 382, 2024
A. Lemaitre & A.-S. Libert, eds.
doi:10.1017/S1743921323004118

Revisiting the Cassini States of synchronous satellites with an angular momentum approach

Alexis Coyette[1], Rose-Marie Baland[2] and Tim Van Hoolst[2]

[1]Naxys Institute, Namur University, Namur, Belgium
email: alexis.coyette@unamur.be

[2]Royal Observatory of Belgium, Brussels, Belgium

Abstract. Like our Moon, the large icy satellites of Jupiter are thought to be in a Cassini State, an equilibrium rotation state characterized by a synchronous rotation rate and a precession rate of the rotation axis equal to that of the normal to the orbit. In these equilibrium states (up to four Cassini States are possible for a solid and rigid satellite), the spin axis of the satellite, the normal to its orbit and the normal to the inertial plane remain coplanar with an obliquity that remains theoretically constant. However, as the gravitational torque exerted on the satellite shows small periodic variations, the orientation of the rotation axis will also vary with time and nutations in obliquity will appear.

Here we present a dynamical model for the study of the Cassini States. This model includes the coupling between the polar motion and the spin axis precession/nutation which is neglected in the classical studies. We study the influence of the triaxiality of Ganymede on its four possible Cassini States, use a Toy model of the Moon to illustrate the nutations in obliquity obtained with the dynamical model, and investigate the influence of the presence of a subsurface ocean on the Cassini State I of Europa.

Keywords. Obliquity, Cassini States, Icy Satellites

1. Cassini States - Definition

The large satellites of our Solar System, like our Moon or the Galilean satellites, are in synchronous rotation, with a period of rotation equal to their period of revolution. This synchronous rotation is often referred to as a Cassini state in reference to Cassini (1693) who described this state of equilibrium for the Moon at the end of the XVII$^{\text{th}}$ century. In this rotation state, the precession rates of both the orbital and equatorial planes are assumed to be constant and equal. Moreover, the spin axis of the Moon, the normal to its orbit and the normal to its Laplace plane are assumed to be coplanar, with a constant obliquity ε (defined as the angle between the normal to the orbit and the spin axis). Due to the precession of the orbit, the orbit normal deviates from the spin axis and the obliquity therefore tends to an equilibrium value for which the torque and the satellite response balances each other. Up to four Cassini states are possible for a biaxial body (Peale 1969).

1.1. *Biaxial case*

By assuming the obliquity to be constant over time, the different Cassini states of a solid and rigid biaxial satellite can be obtained from the following classical equation (see e.g. Colombo (1966); Ward and Hamilton (2004))

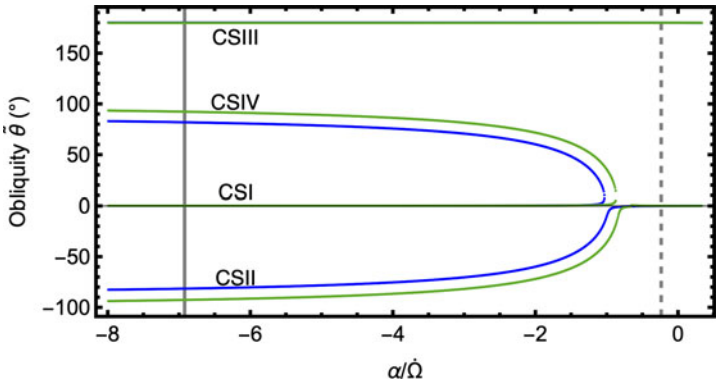

Figure 1. Cassini States of a biaxial (blue) and triaxial (green) Ganymede for different values of $\alpha/\dot{\Omega}$ ranging from -8 to 0.5. For the actual value of $\alpha/\dot{\Omega}$, indicated by the vertical black lines, four Cassini States are possible. If Ganymede were to have a ratio $\alpha/\dot{\Omega}$ similar to that of the Moon (see vertical dashed lines), only two Cassini States would be possible.

$$\alpha_{\rm bi}\sin[2(\tilde{\theta}-i)]+2\dot{\Omega}\sin\tilde{\theta}=0. \tag{1}$$

In this equation, $\alpha_{\rm bi}=\frac{3}{2}\frac{C-\overline{A}}{C}n$ is the frequency of the Free Precession, with n the mean motion of the satellite and $\overline{A}$ and C are the mean equatorial and polar moments of inertia of the biaxial satellite, respectively ($\overline{A}<C$). $\tilde{\theta}$ is the angle between the figure axis and the normal to the inertial plane, or inertial obliquity angle, and $\dot{\Omega}$ the frequency of the precession which is retrograde ($\dot{\Omega}<0$) for the Galilean satellites and the Moon. In these classical studies, the gravitational torque exerted by the central planet is averaged over short period terms. Morevover, the polar motion is neglected so that the rotation axis is assumed to be aligned with the figure axis. We therefore denote this obliquity by $\tilde{\theta}$ to make the distinction between this figure axis inertial obliquity and the spin axis inertial obliquity θ. Obliquities measured from the orbit axis are denoted similarly $\tilde{\varepsilon}=(\tilde{\theta}-i)$ and $\varepsilon=(\theta-i)$, with i the constant orbital inclination with respect to the Laplace plane.

For satellites like the Galilean moons, with a slow orbital precession in comparison with the free precession (i.e. $|\dot{\Omega}|\ll\alpha$), Eq. (1) possesses four solutions characterized by an obliquity close to 0 (Cassini State I, CSI), $-\frac{\pi}{2}$ (CSII), π (CSIII), and $\frac{\pi}{2}$ (CSIV), see Fig. 1. For a satellite characterized by a short orbital precession period (i.e. $|\dot{\Omega}|\gg\alpha$), however, the first term of Eq. (1) can be neglected in front of the second term and we are then left with only two possible Cassini States (CSII and CSIII, with obliquities close to zero and π, respectively, see Fig. 1). This is the case for our Moon that is considered to be in Cassini State II (see e.g. Beletskii 1972; Ward 1975; Henrard and Schwanen 2004).

1.2. *Triaxial case*

The classical equation describing the different Cassini states of a rigid and solid traxial satellite is (see e.g. Ward 1975)

$$\alpha_{\rm tri}\sin[2(\tilde{\theta}-i)]+\frac{3}{4}n\frac{B-A}{C}\sin(\tilde{\theta}-i)\left[1-\cos(\tilde{\theta}-i)\right]+2\dot{\Omega}\sin\tilde{\theta}=0, \tag{2}$$

where $\alpha_{\rm tri}=\frac{3}{2}n\frac{C-A}{C}$ is the frequency of the Free Precession of the triaxial body and $A<B<C$ are the principal moments of inertia of the triaxial satellite. The obliquities obtained for Cassini States I and III are very close to the ones for a biaxial satellite. However, for a large orbital precession period in comparison with the period of the Free

https://doi.org/10.1017/S1743921323004118 Published online by Cambridge University Press

Table 1. Figure axis obliquities $\tilde{\theta}$ for a biaxial (Eq. 1) or triaxial (Eq. 2) Ganymede.

	biaxial	**triaxial**
$\tilde{\theta}_{\rm I}^{\rm Cl}$ (°)	0.238	0.213
$\tilde{\theta}_{\rm II}^{\rm Cl}$ (°)	−76.543	−92.827
$\tilde{\theta}_{\rm III}^{\rm Cl}$ (°)	180.148	180.148
$\tilde{\theta}_{\rm IV}^{\rm Cl}$ (°)	76.908	93.196

Precession, the Cassini States II and IV present a strong deviation due to the triaxiality of the body (deviation of 16° for Ganymede, see Tab. 1).

2. Our dynamical model

The classical equations (Eqs. 1-2) overlook the possibility of time variations (or nutations) in obliquity and in longitude induced by the time-varying gravitational torque acting on the satellite. Here, we use dynamical equations with a non averaged torque to study the behaviour of the obliquity. Our model also couples the spin axis precession/nutation in space with the smaller polar motion, which was neglected in the classical studies. It is described by means of two equations:

(1) The Angular Momentum equation stating that the time derivative of the angular momentum $\vec{H}$ is equal to the applied torque $\vec{\Gamma}$ (Eckhardt 1981)

$$\frac{d\vec{H}}{dt} + \vec{\Omega} \times \vec{H} = \vec{\Gamma}, \tag{3}$$

where $\vec{\Omega} = n(m_X(t), m_Y(t), 1 + m_Z(t))$ is the rotation vector of the satellite and where the angular momentum $\vec{H}$ is given by the product of the inertia tensor and the rotation vector

$$\vec{H} = \begin{pmatrix} A & 0 & 0 \\ 0 & B & 0 \\ 0 & 0 & C \end{pmatrix} \cdot \vec{\Omega}. \tag{4}$$

(2) The equation describing the invariance of the Laplace Pole in inertial space:

$$\frac{d\hat{p}}{dt} + \vec{\Omega} \times \hat{p} = 0, \tag{5}$$

where $\hat{p} = (p_X(t), p_Y(t), p_Z(t))$ is the unit vector along the normal to the Laplace plane.

These equations are written in the Cartesian coordinates of the Body Frame (BF) of the satellite and split into a system of 4 dynamical equations with 4 unknowns $m_X(t)$, $m_Y(t)$, $p_X(t)$ and $p_Y(t)$ (see also Baland et al. (2019)):

$$(C - B)n^2 m_Y(t) + Anm'_X(t) = \Gamma_X(t) \tag{6a}$$

$$(A - C)n^2 m_X(t) + Bnm'_Y(t) = \Gamma_Y(t) \tag{6b}$$

$$-np_Y(t) + nm_Y(t)p_Z(t) + p'_X(t) = 0 \tag{6c}$$

$$np_X(t) - nm_X(t)p_Z(t) + p'_Y(t) = 0. \tag{6d}$$

Note that a fifth variable ($p_Z(t)$) appears in these equations. In Cassini State I (resp. CSIII), the obliquity is close to zero (resp. π) so that the normal to the Laplace plane can be approximated by $\hat{p} \approx (p_X(t), p_Y(t), 1)$ (resp. $\hat{p} \approx (p_X(t), p_Y(t), -1)$). In the following, we analytically solve the system of equations (6a-6d) in the case of the Moon and obtain the time-varying equatorial components of the polar motion ($m_X(t), m_Y(t)$) and of the

https://doi.org/10.1017/S1743921323004118 Published online by Cambridge University Press

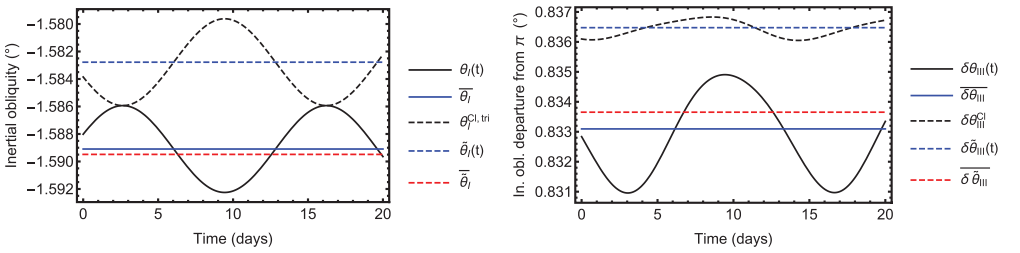

Figure 2. Left panel: CSI inertial obliquities $\theta_{\rm I}(t)$ and $\tilde{\theta}_{\rm I}(t)$ as a function of time for the Moon (solid and dashed black lines, respectively). Right-panel: CSIII departure from π in inertial obliquities $\theta_{\rm III}(t)$ and $\tilde{\theta}_{\rm III}(t)$ as a function of time for the Moon (solid and dashed black lines, respectively) The blue solid and dashed lines represent the mean values of the inertial obliquities (CSI) and of the inertial obliquity departure from π (CSIII). The red dashed lines represent the constant-over-time results of the Classical model (Eq. 2).

Laplace pole motion $(p_X(t), p_Y(t))$. The figure axis inertial obliquity $\tilde{\theta}_{\rm I}(t)$ (resp. $\tilde{\theta}_{\rm III}(t)$) and the spin axis inertial obliquity $\theta_{\rm I}(t)$ (resp. $\theta_{\rm III}(t)$) are then obtained as byproducts (see Coyette et al. (2023), in prep.).

2.1. *Cassini State I*

Even if the Moon is formally considered to be in the Cassini State II due to its short orbital precession period compared to its free precession period (Ward 1975), its obliquity can be obtained from the small-angle approximation and therefore by the same formulae used here for the Cassini State I. We obtain mean inertial obliquities values of $\overline{\theta}_{\rm I} = -1.589°$ and $\overline{\tilde{\theta}}_{\rm I} = -1.583°$ (see Fig. 2, left panel, blue lines), close to the value obtained with the classical "triaxial" equation (red line). The slight difference between the "dynamical" $\overline{\tilde{\theta}}_{\rm I}$ and the "classical" $\tilde{\theta}_{\rm I}^{\rm Cl,tri}$ values is due to the coupling between the polar motion and the spin precession. The nutations in obliquity of the spin and figure axes have an amplitude of 11 arcsec and are both semi-diurnal and 180° out of phase from each other (black lines). The spin axis and the figure axis are confounded two times per day as the polar motion semi-diurnally vanishes (see Coyette et al. (2016)).

Note that $\overline{\theta}_{\rm I}$ and $\overline{\tilde{\theta}}_{\rm I}$ differ from the obliquity observed by lunar laser ranging observations (Dickey et al. 1994, $-1.543°$), likely because of the assumptions made here. In particular we assume a rigid satellite and the small-angle approximation, as in Dumberry and Wieczorek (2016). Note also that neglecting the solar torque acting on the Moon in the Cassini State model leads to a discrepancy with respect to observations, Stys and Dumberry (2018). We do not aim to reproduce the observed value and the results presented here for the Moon should only be considered as those of a Toy Model intended to discuss the semi-diurnal nutations in obliquity and the coupling between the polar motion and the spin precession/nutation in the case of a satellite precessing at constant rate.

2.2. *Cassini State III*

We here hypothetically assume that the Moon is in Cassini State III and model its time-varying spin and figure axes inertial obliquities. The inertial obliquity departures $\delta\theta_{\rm III}(t) = \theta_{\rm III}(t) - \pi$ and $\delta\tilde{\theta}_{\rm III}(t) = \tilde{\theta}_{\rm III}(t) - \pi$ are presented on Fig. 2 (right panel, black lines). The mean inertial obliquities are $\overline{\theta}_{\rm III} = 180.833°$ and $\overline{\tilde{\theta}}_{\rm III} = 180.836°$, respectively (blue lines). Similarly as for CSI, the value of $\overline{\tilde{\theta}}_{\rm III}$ is close but not equal to the value $\tilde{\theta}_{\rm III}^{\rm Cl,tri}$ derived with the classical equations (red line), due to the coupling between the polar motion and the spin precession that is here fully considered.

https://doi.org/10.1017/S1743921323004118 Published online by Cambridge University Press

The nutations in obliquities are the superimposition of two semi-diurnal terms with amplitudes of 1.3 and 6.0 arcsec and of one quarter-diurnal term with an amplitude of 0.7 arcsec. In CSIII, the polar motion never vanishes so that the spin axis and the figure axis always point toward different directions.

3. Influence of a subsurface ocean

Many large icy satellites of the Solar System likely possess a global ocean beneath a thin ice shell. Such an ice shell is sometimes assumed to be mechanically decoupled from the solid interior and to precess somewhat independently, with an obliquity larger than that of an entirely solid and rigid body (e.g. Bills and Nimmo 2008, 2009 for the case of Titan, see also Chen et al. (2014); Nimmo (2023)). Baland et al. (2011) drawn a different conclusion and argued that the observed large obliquity of Titan (0.3°, Stiles et al. 2008; Meriggiola et al. 2016, about three times the value expected for an entirely solid Titan) is explained by a resonant amplification of the obliquity of the shell which is partially mechanically coupled to the interior. Baland et al. (2012) also found that the obliquity can be smaller than that of an entirely solid satellite, due to a lack of such a resonance, as could be the case for Europa. We revisit below the obliquity of the shell of Europa, starting from the coupled model of Baland et al. (2019).

3.1. *Equations*

To model the influence of the ocean on the obliquity, we consider one angular momentum equation for each layer k of the satellite (shell s, ocean o and interior i), expressed in the Cartesian coordinates of the BF of that layer if it is solid, or of the BF of the shell in the case of the ocean:

$$\frac{d}{dt}\vec{H}_k + \vec{\Omega}_k \times \vec{H}_k = \vec{\Gamma}_k, \tag{7}$$

where $\vec{\Gamma}_k$ is the total torque applied on layer k that includes the external gravitational torque exerted by the central planet, the internal gravitational and pressure torques exerted by the other layers, including the inertial torque due to the Poincaré flow inside the subsurface ocean. We also use the equations stating the invariance of the Laplace Pole, expressed in the BF of both solid layers (shell s and interior i)

$$\frac{d\hat{p}_k}{dt} + \vec{\Omega}_k \times \hat{p}_k = 0. \tag{8}$$

We then analytically solve Eqs. (7-8) to obtain the polar motion components $(m_{X,k}, m_{Y,k})$ of the different internal layers of the satellite ($k = i$, $k = o$ or $k = s$) as well as the Laplace pole components $(p_{X,k}, p_{Y,k})$ for the two solid layers ($k = i$ or $k = s$) and compute the obliquity of the shell.

3.2. *Numerical results*

The mean orbital obliquity $\bar{\varepsilon}$ of the shell of Europa is presented on Fig. 3 for a large set of possible interior models of Europa compatible with the observed mass, radius and moment of inertia. We first model the obliquity of Europa without considering the inertial torque (similarly as was done by Baland et al. (2012), their Fig. 5). In this case, the obliquity increases from 0.027° to 0.039° with increasing ice shell thickness (left panel of Fig. 3), and is smaller than the expected obliquity of an entirely solid Europa (0.055°). These obliquities are about 0.005° smaller than those obtained by Baland et al. (2012) as the value we use here for the mass of Europa slightly differs from the value used in this paper.

https://doi.org/10.1017/S1743921323004118 Published online by Cambridge University Press

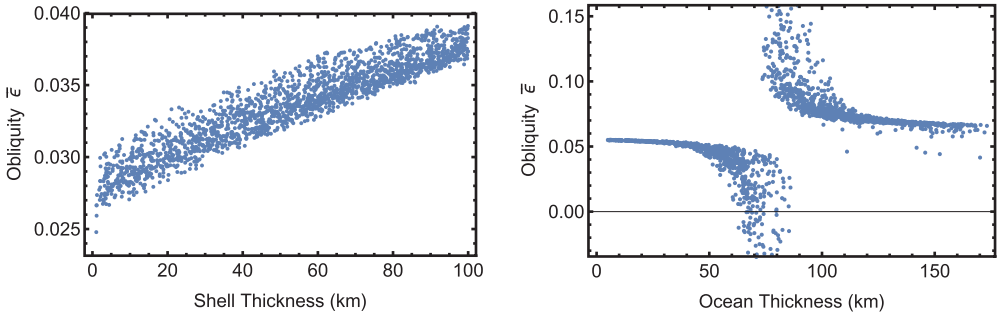

Figure 3. Mean obliquity of Europa's shell for a large set of interior models, without inertial coupling and as a function of the ice shell thickness (left panel), and with inertial coupling and as a function of the ocean thickness (right panel).

We note that the obliquity of Europa's shell is strongly influenced by the inertial torque due to the Poincaré flow inside the subsurface ocean. Due to a resonance with a free mode associated with the presence of the ocean (the Free Ocean Nutation), the mean obliquity of the shell of Europa is either amplified to values as large as 0.15° or decreased to values closer to zero, for models with an ocean thickness ranging from 50 to 120 km. For models far away from this resonance, the obliquity of the shell of Europa is similar to the obliquity of 0.055° expected for an entirely solid satellite.

4. Conclusion

We here introduce a dynamical model based on an angular momentum approach for the study of the Cassini States I and III of large synchronous satellites. Since we do not average the gravitational torque exerted on the satellite, the nutations in obliquity and in longitude can be studied from this model, whereas they were neglected in the Classical Cassini states models (see e.g. Colombo (1966),Ward (1975)). Moreover, the coupling between the spin axis precession and the polar motion is fully included in our model.

Our dynamical model shows good agreement with the classical solutions derived for CSI and CSIII, the slight difference being due to the coupling between the polar motion and the spin axis precession.

With presence of a subsurface ocean at rest, the obliquity of the shell of Europa is smaller than the obliquity obtained for a entirely solid satellite. If we add the inertial torque caused by a Poincaré flow inside the subsurface ocean in our model, depending on the ocean thickness, the obliquity of Europa ranges between 0 and a few tens of degrees. Far from a resonance with the Free Ocean Nutation, the obliquity remains close to the obliquity of an entirely solid satellite. Those results are in contradiction with the assumption that the obliquity of the shell of a satellite with an internal global ocean should necessarily be larger than that of an entirely solid satellite.

Acknowledgment

This work was financially supported by the Belgian PRODEX program managed by the European Space Agency in collaboration with the Belgian Federal Science Policy Office.

References

Baland, R.-M., Coyette, A., & Van Hoolst, T. 2019, *Celestial Mechanics and Dynamical Astronomy*, 131(2), 11.

Baland, R. M., Van Hoolst, T., Yseboodt, M., & Karatekin, Ö. 2011, *A&A*, 530, A141.

Baland, R.-M., Yseboodt, M., & Van Hoolst, T. 2012, *Icarus*, 220, 435–448.

https://doi.org/10.1017/S1743921323004118 Published online by Cambridge University Press

Beletskii, V. V. 1972, *Celestial Mechanics*, 6(3), 356–378.
Bills, B. & Nimmo, F. In *European Planetary Science Congress* 2009, 553.
Bills, B. G. & Nimmo, F. 2008, *Icarus*, 196(1), 293–297.
Cassini, J. 1693,. *De l'Origine et du progrès de l'Astronomie et de son usage dans la Gèographie et dans la navigation.*
Chen, E. M. A., Nimmo, F., & Glatzmaier, G. A. 2014, *Icarus*, 229, 11–30.
Colombo, G. 1966, *The Astronomical Journal*, 71(9), 891–896.
Coyette, A., Baland, R.-M., & Van Hoolst, T. 2023, *in preparation.*
Coyette, A., Hoolst, T. V., Baland, R.-M., & Tokano, T. 2016, *Icarus*, 265, 1 – 28.
Dickey, J. O., Bender, P. L., Faller, J. E., *et al.* 1994, *Science*, 265(5171), 482–490.
Dumberry, M. & Wieczorek, M. A. 2016, *JGR: Planets*, 121(7), 1264–1292.
Eckhardt, D. H. 1981, *Moon and Planets*, 25(1), 3–49.
Henrard, J. & Schwanen, G. 2004, *Celestial Mechanics and Dynamical Astronomy*, 89(2), 181–200.
Meriggiola, R., Iess, L., Stiles, B. W., *et al.* 2016, *Icarus*, 275, 183–192.
Nimmo, F. In *Uranus Flagship: Investigations and Instruments for Cross-Discipline Science Workshop* 2023, 8009.
Peale, S. J. 1969, *The Astronomical Journal*, 74(3), 483–489.
Stiles, B. W., Kirk, R. L., Lorenz, R. D., *et al.* 2008, *The Astronomical Journal*, 135(5), 1669–1680.
Stys, C. & Dumberry, M. 2018, *JGR: Planets*, 123, 2868–2892.
Ward, W. R. 1975, *The Astronomical Journal*, 80(1), 64–70.
Ward, W. R. & Hamilton, D. P. 2004, *The Astronomical Journal*, 128(5), 2501–2509.